frontiers in Physiology

ORIGINAL RESEARCH
published: 09 May 2019
doi: 10.3389/fphys.2019.00556

Honey Bee Parasitic Mite Contains the Sensilla-Rich Sensory Organ on the Foreleg Tarsus Expressing Ionotropic Receptors With Conserved Functions

*Jing Lei, Qiushi Liu and Tatsuhiko Kadowaki**

Department of Biological Sciences, Xi'an Jiaotong-Liverpool University, Suzhou, China

Honey bee parasitic mites (*Tropilaelaps mercedesae* and *Varroa destructor*) detect temperature, humidity, and odor but the underlying sensory mechanisms are poorly understood. To uncover how *T. mercedesae* responds to environmental stimuli inside a hive, we first identified the sensilla-rich sensory organ on the foreleg tarsus. The organ appeared to correspond to Haller's organ in ticks and contained four types of sensilla, which may respond to different stimuli based on their morphology. We searched for differentially expressed genes between the forelegs and hindlegs to identify mRNAs potentially associated with the sensory organ. The forelegs were enriched with mRNAs encoding sensory proteins such as ionotropic receptors (IRs) and gustatory receptors, as well as proteins involved in ciliary transport. We also found that *T. mercedesae* IR25a and IR93a were capable of rescuing temperature and humidity preference defects in *Drosophila melanogaster IR25a* and *IR93a* mutants. These results demonstrate that the structures and physiological functions of ancient IRs have been conserved during arthropod evolution. Our study provides insight into the sensory mechanisms of honey bee parasitic mites, as well as potential targets for methods to control the most serious honey bee pest.

Keywords: honey bee decline, sensory organ, honey bee parasitic mite, ionotropic receptors, ciliary transport

OPEN ACCESS

Edited by:
Monique Gauthier, Université Toulouse III Paul Sabatier, France

Reviewed by:
Marcus Carl Stensmyr, Lund University, Sweden
Philippe Lucas, Institut National de la Recherche Agronomique (INRA), France
Juan Antonio Sánchez-Alcañiz, Université de Lausanne, Switzerland

***Correspondence:**
Tatsuhiko Kadowaki
Tatsuhiko.Kadowaki@xjtlu.edu.cn

Specialty section:
This article was submitted to Invertebrate Physiology, a section of the journal Frontiers in Physiology

Received: *21 January 2019*
Accepted: *24 April 2019*
Published: *09 May 2019*

Citation:
Lei J, Liu Q and Kadowaki T (2019) Honey Bee Parasitic Mite Contains the Sensilla-Rich Sensory Organ on the Foreleg Tarsus Expressing Ionotropic Receptors With Conserved Functions. Front. Physiol. 10:556. doi: 10.3389/fphys.2019.00556

INTRODUCTION

The number of managed honey bee colonies has declined across North America and Europe in recent years (Goulson et al., 2015). Pollination by honey bees is critical for maintaining ecosystems and producing many agricultural crops (Klein et al., 2007; Aizen and Harder, 2009). Prevention of honey bee losses has, therefore, become a major issue in apiculture and agriculture. Although there are many potential causes for the observed declines, ectoparasitic mites are considered to be major threats to the health of honey bees and their colonies (Evans and Schwarz, 2011; Goulson et al., 2015). *Varroa destructor* is present globally (except Australia) and causes both abnormal brood development and brood death in honey bee colonies (Rosenkranz et al., 2010). The mites feed on hemolymph and also spread honey bee viruses, particularly deformed wing virus (DWV) (de Miranda and Genersch, 2010; Martin et al., 2012). In many Asian countries,

another honey bee ectoparasitic mite, *Tropilaelaps mercedesae*, is also prevalent in *Apis mellifera* colonies (Anderson and Morgan, 2007; Luo et al., 2011). These two emerging parasites of *A. mellifera* share many characteristics (Anderson and Roberts, 2013). For example, they have similar reproductive strategies (Sammataro et al., 2000) and both are vectors for DWV (Yue and Genersch, 2005; Dainat et al., 2009; Forsgren et al., 2009; Wu et al., 2017). As a result, *T. mercedesae* or *V. destructor* infestations have similar negative impacts on *A. mellifera* colonies (Dainat et al., 2012; Khongphinitbunjong et al., 2016; Nazzi and Le Conte, 2016). Although *T. mercedesae* is currently restricted to Asia, it has the potential to spread and establish worldwide due to the global trade in honey bees.

Varroa destructor prefers temperatures of 32 ± 2.9°C, reproduces best at 32.5–33.4°C, and has been shown to discriminate temperature differences of 1°C (Le Conte and Arnold, 1987, 1988; Le Conte et al., 1990). Furthermore, its reproduction also depends on humidity of 55–70% (Nazzi and Conte, 2016). These results demonstrate thermo- and hygrosensation of *V. destructor* play important roles to adapt to the honey bee hive environment; nevertheless, chemoreception must be most important in the various interactions between mites and their honey bee hosts. For example, *V. destructor* prefers to parasitize nurse bees rather than foragers during its phoretic phase (Kraus, 1993; Xie et al., 2016). For its reproductive stage, it locates fifth instar honey bee larva and enters the brood cell prior to capping (Aumeier et al., 2002). These behaviors are considered to be mediated by chemical cues derived from the adult bee, larva, and larval food. Since *T. mercedesae* has a very similar life cycle to *V. destructor*, both honey bee mites should be equipped with thermo-, hygro-, and chemosensation, as observed in other mite/tick (Acari) species. Accordingly, *V. destructor* was found to have a sensilla-rich sensory organ on the foreleg tarsus (Dillier et al., 2006; Häußermann et al., 2015), which corresponds to Haller's organ in ticks (Belozerov et al., 1997). Proteomic and transcriptomic characterization were conducted for the forelegs of *V. destructor,* which identified potential semiochemical carriers and sensory proteins (Iovinella et al., 2018).

Ionotropic receptors (IRs) represent a subfamily of ionotropic glutamate receptors (iGluRs), which are conserved ligand-gated ion channels. IRs have specifically evolved in protostomes (Croset et al., 2010) and are best characterized in the fruit fly, *Drosophila melanogaster*. Most IRs are expressed in sensory neurons and function as chemoreceptors to detect various odorants and tastants (Benton et al., 2009; Rytz et al., 2013). Recent studies have also demonstrated that IR21a, IR40a, IR68a, IR93a, and IR25a are critical for thermo- and hygrosensation, suggesting that IRs have diverse physiological roles as well as gating mechanisms (Enjin et al., 2016; Knecht et al., 2016; Ni et al., 2016; Frank et al., 2017). IR25a has the same protein domains as iGluRs, is expressed broadly in various sensory neurons, and is deeply conserved in protostomes. These findings suggest that IR25a is likely to function as a co-receptor with other IRs, similar to the Orco pairing with other olfactory receptors (ORs).

In this study, we aimed to identify and characterize a sensilla-rich sensory organ in *T. mercedesae* using scanning electron microscopy (SEM). By comparing the transcriptomes of forelegs and hindlegs (the second to fourth legs), we identified potential genes that may be highly expressed in the sensory organ. Identification of this major sensory organ and its associated proteins in *T. mercedesae* inform our understanding of the mechanisms of sensory perception in honey bee parasitic mites.

MATERIALS AND METHODS

Mite Sampling

Tropilaelaps mercedesae infested honey bee colonies were obtained from a local beekeeper in Suzhou, China. Adult females of *T. mercedesae* were collected from the capped brood cells and dissected under a light microscope using fine forceps. The collected mites were directly used for all experiments and kept together with honey bee pupae in 33°C incubator when necessary.

SEM

A cold field emission gun SEM (Hitachi S-4700, Hitachi Company) was used for characterizing sensory organs of *T. mercedesae*. The whole mites and dissected legs were sprayed with gold alloy first, and then mounted on a conductive adhesive tape. During the observation, each sensillum was assigned with a number to classify the types of sensilla.

RNA-Seq

Total RNA was extracted from the forelegs, hindlegs, and main bodies of 50 adult females of *T. mercedesae* using TRI Reagent (Sigma). High-quality RNA samples in duplicate were then sequenced at BGI (Shenzhen, China) using Illumina HiSeq 4000 platform. After sequencing, the raw data were filtered to remove the adaptor sequences, contamination, and low-quality reads by BGI. The quality control (QC) was further analyzed using FastQC. All RNA-seq data are available in SRA database with the accession #: PRJNA510306.

Bioinformatics

The reference genome and annotated genes of *T. mercedesae* were first acquired from NCBI[1], and then used for building the index by Hisat2–build indexer (Kim et al., 2015). The generated index files were used to align the clean reads of six RNA-seq samples to the reference genome. Subsequently, SAM file outputs from the previous step were sorted using SAMtools (Li et al., 2009). HTSeq-count (Anders et al., 2015) was further applied to obtain the raw read counts for downstream analysis of identifying the DEGs in *R* (V3.4.3) based Bioconductor edgeR package (V3.20.9) (Robinson et al., 2010). DEGs were cut-off by a false discovery rate (FDR) at 0.05, and then they were subjected to gene ontology (GO) term enrichment analysis using Blast2GO (Conesa et al., 2005). The results of GO enrichment analysis between the forelegs, hindlegs as well as main bodies were cut-off by FDR at 0.05.

[1]https://www.ncbi.nlm.nih.gov/genome/53919?genome_assembly_id=313451

TmIR25a and *TmIR93a* cDNA Cloning

For *TmIR25a* and *TmIR93a*, the full length cDNAs were obtained by identifying the 5′ and 3′ ends with RACE method. To amplify 5′ end sequence of *TmIR25a*, the following two primers: 5′-GAG TGTTTGTCCAAGTACATTCTCGA-3′ (first PCR) and 5′-AGT GTTATCACAAGGAGATATGAGATC-3′ (second PCR) were used for 5′RACE with SMART RACE kit (TAKARA). The 3′ end sequence was determined by 3′RACE using the following two primers: 5′-CCATCAAGAACATCGGTGGTG-3′ (first PCR) and 5′-GGCCTGCATCACATTAGTGTTC-3′ (second PCR). 5′RACE for *TmIR93a* was conducted with two primers, 5′-ATCGAGTGC GATCACAAGCAG-3′ (first PCR) and 5′-ACTCTCAGATT CCGGATTCACC-3′ (second PCR) using 5′-Full RACE Kit (TAKARA). For the 3′ RACE, following two primers: 5′-GGGCAAACAGGTTACAGCTTC-3′ (first PCR) and 5′-CC CCAACAGGACCGATCTTAT-3′ (second PCR) were used. *TmIR25a* full length cDNA was amplified by nested PCR using the following primer sets: Forward-5′-GCGTGAACACATC AGGCCGCT-3′ and Reverse-5′-CCCACTCGGAACTTCGTGT CG-3′ (first PCR), Forward-5′-TTTGCGGCCGCT**ATG**TGGGT CCCTTTACGGATCTC-3′ and Reverse-5′-TTTTCTAGACTTT TCTTTTGTGGCATGTGGTCTTTC-3′ (second PCR). Similarly, *TmIR93a* full length cDNA was obtained using the following primer sets: Forward-5′-GGGAGAAAGCCGAGCT GGTAA-3′ and Reverse-5′-TTGTGAATGTCGCCGGTATCC-3′ (first PCR), Forward-5′-TTTGCGGCCGCGAC**ATG**TGGCCTC GACTCATATTT-3′ and Reverse-5′-TTTTCTAGACTGTATCG CCTGGCGGGGTAGTT-3′ (second PCR). The PCR products were digested by NotI and XbaI and cloned into pAc5.1/V5-His vector (Thermo Fisher Scientific) in which *Drosophila melanogaster Act5C* promoter was replaced by CMV promoter for expression of the V5-epitope tagged proteins in HEK293 cells. To generate *UAS-TmIR25a* and *UAS-TmIR93a* transgenic fruit flies, the untagged versions of above expression constructs were first prepared. The EcoRI-XbaI fragment of *TmIR25a* in above construct was replaced with the restriction enzyme digested PCR product obtained with two primers, 5′-GCCAC GATGACCAACTGTGAT-3′ and 5′-CGGGCCCTCTAGA**CTA**T TTCTT-3′. The HindIII-XbaI fragment of *TmIR93a* was replaced with the restriction enzyme digested PCR product obtained with two primers, 5′-GGCCAAGCGGTCATCGAGATA-3′ and 5′-GC CCTCTAGA**CTA**GTATCGCCT-3′. The untagged cDNAs were then cloned in pUASTattB (Brand and Perrimon, 1993) digested with NotI and XbaI. The accession numbers for *TmIR25a* and *TmIR93a* are LC438511 and LC438512, respectively.

Western Blot

HEK293 cells in 12-well plate were transfected with 1 μg of above expression construct (the V5-epitope tagged version) using 2 μL of Lipofectamine 2000 under OPTI-MEM medium (Thermo Fisher Scientific) for 24 h. The transfected cells were washed once with PBS, and then lysed with 200 μL of SDS-PAGE sample buffer. The cell lysates were sonicated and heated at 60°C for 5 min. The proteins were separated by 8% SDS-PAGE and transferred to a NC membrane (PALL, 66485) by Pierce 2 Fast Blotter (Thermo Fisher Scientific, B103602038). The membrane was first blocked with 5% BSA/TBST (10 mM Tris-HCl, 150 mM NaCl, and 0.1% Tween 20) for 40 min, and then incubated with rabbit anti-V5-epitope antibody (SIGMA) (1:1,000) for 2 h at room temperature. The membrane was washed with TBST for five times (5 min each), and then incubated with IRDye800-conjugated secondary antibody (LI-COR) (1:10,000) for 1.5 h at room temperature under dark and washed as above. The fluorescent signal was detected by Odyssey (LI-COR).

Fruit Fly Genetics

UAS-TmIR25a and *UAS-TmIR93a* prepared above were integrated at attP2 site on third chromosome. Stocks of *IR25a-GAL4* (BDSC 41728), $IR25a^2$ (BDSC 41737), *UAS-IR25a* (BDSC 41747), and $IR93a^{MI05555}$ (BDSC 42090) were obtained from Bloomington Drosophila Stock Center (BDSC). Using above stocks, we generated $IR25a^2$ *UAS-IR25a,* $IR25a^2$ *IR25a-GAL4,* $IR25a^2$*; UAS-TmIR25a, IR25a-GAL4;* $IR93a^{MI05555}$, and $IR93a^{MI05555}$ *UAS-TmIR93a* stocks. The appropriate crosses were made between *Gal4* and *UAS* stocks to test whether *TmIR25a* or *TmIR93a* can rescue the behavioral defects of *IR25a* or *IR93a* mutant.

Thermotaxis Test

To assay the temperature preference of fruit flies, a temperature gradient of 10–40°C with a slope of 1.07°C/cm was produced in an aluminum block (27 long × 15 wide × 2.5 cm high) as previously reported (Sayeed and Benzer, 1996). The temperature gradient was established using a cold circulating water chamber and a hot probe at each end. The aluminum block was covered with moist paper to maintain a uniform relative humidity (RH) along the gradient. This paper was divided into 20 observation fields with a black pencil for recording the distribution of fruit flies. A glass plate with three separate lanes was placed 5 mm above the block, creating suitable corridors for fruit flies to migrate. Approximately 30 adult flies (4–5 days old) per lane were placed in the middle of testing arena around 25°C between the aluminum block and the glass plate, allowed to migrate for 3 h, and photographed every 10 min with a digital camera. When the positions of fruit flies in the apparatus were stabilized between 1.5 and 2.5 h (This time period did not differ between the experimental groups), the number of fruit flies located at the area <24°C was counted. Preference index was calculated by the number of flies at <24°C/the total number of flies. The preference indexes of all tested groups were statistically analyzed by one-way ANOVA with multiple comparisons followed by Dunnett test. In each test, wild type, mutant, and the rescued fruit flies were examined simultaneously. All experiments were performed in a room where the temperature was kept constant at 25°C.

Thermotaxis of *T. mercedesae* was tested as above except with 15–40°C gradient or without temperature gradient. The testing arena was photographed every 10 min for 1h and we counted the number of mites located at the area >32°C followed by calculating the preference index as above. The mites distributed evenly in the testing arena without temperature gradient and we counted the number of mites in the same area as we did with 15–40°C gradient.

Humidity Preference Test

Hygrosensory behavior was assayed as previously reported (Enjin et al., 2016). A 12-well cell culture plate was modified to make a well-defined chamber with two spaces. A half of wells was filled with saturated solution of LiCl (20% humidity at 25°C) while another half was filled with saturated NaCl (70% humidity at 25°C) to maintain stable RH on the liquid surface in an enclosed space. The plate was then covered by a nylon mesh and closed with a lid matching the plate. In each test, approximately 80 adult flies (4–5 days old) were briefly ice anesthetized and placed at the center of apparatus. The lid was sealed to stabilize RH inside the apparatus. Humidity preference of the fruit flies with different genotypes was recorded using a digital camera and the number of flies on each side was recorded manually at 3–5 h after the start of recording. Humidity preference index was calculated by (the number of flies on NaCl side – the number of flies on LiCl side)/total number of flies. The preference indexes of all tested groups were statistically analyzed by one-way ANOVA with multiple comparisons followed by Dunnett test.

Humidity preference of *T. mercedesae* was tested as above except saturated NaCl was replaced with H_2O (96% humidity at 25°C). The control experiment using 12-well cell culture plate filled with H_2O was also carried out. The number of mites on each side was counted every 10 min for 1 h and we calculated the preference index as above.

RESULTS

Identification of a Sensilla-Rich Sensory Organ on the Foreleg Tarsus of *T. mercedesae*

We observed the forelegs and hindlegs of *T. mercedesae* using SEM and found that only the foreleg tarsus contained a putative sensory organ on the dorsal side, with more than 20 sensilla of various shapes and sizes (**Figures 1A–D**). Most of the sensilla were equipped with well-defined sockets (**Figure 1A**). We characterized the shape of each sensillum at high magnification and found that they could be classified into four different types based on the shape: type 1 had a rough surface with many indentations, sensillum #3 (**Figure 1F**), type 2 had a terminal pore, sensillum #18 (**Figure 1G**), type 3 included 18 sensilla with smooth surface, e.g., sensillum #8 (**Figure 1H**), and type 4 had surface pores at various densities—sensilla #2, #7/#12, #10 had pores at high, medium, and low density, respectively (**Figures 1I–K**). Several long sensilla were found on all legs and these are likely to be mechanosensory bristles. The pedipalp of *T. mercedesae* also contains a cluster of sensilla at the distal end (**Figure 1E**); however, all of them have smooth surface (**Figure 1L**).

Identification of Potential mRNAs Enriched With the Sensory Organ

To identify potential mRNAs highly expressed in the sensory organ, we obtained RNA-seq reads from the forelegs, hindlegs, and main bodies (without legs) and then identified the differentially expressed genes (DEGs) between the forelegs and hindlegs. Since only foreleg tarsi were equipped with the sensory organs, we expected the DEGs to represent the sensory organ-associated mRNAs. We found that 46.1–83.9% of the sequence reads were aligned with the *T. mercedesae* genome (**Supplementary Table S1**) and we used these to identify DEGs between the forelegs and hindlegs, the forelegs and main bodies, and the hindlegs and main bodies. The lists of DEGs are shown in **Supplementary Tables S2–S4**. **Table 1** and **Supplementary Tables S5**, **S6** indicate GO terms enriched for the genes highly expressed in the forelegs compared to the hindlegs and main bodies, and the ones highly expressed in the hindlegs relative to the main bodies, respectively. For the genes highly expressed in the forelegs, many of the GO terms were associated with ion channel activity, particularly iGluR activity, as well as microtubule motor activity in the "molecular function" category. In the "biological process" category, GO terms related to cilium assembly, microtubule-based processes, and detection of chemical stimulus involved in sensory perception were most prevalent. All GO terms in the "cellular component" category were related to cilium, intraciliary transport particle, and BBSome (**Table 1**). Several GO terms related to mitochondrial activity were also enriched in the forelegs, compared with the main bodies, and this was similar for the genes highly expressed in the hindlegs relative to the main bodies (**Supplementary Tables S5**, **S6**). These results are consistent with the finding that the sensory organ on the foreleg tarsus had many sensilla (**Figure 1**) and with the ciliated sensory neurons and the expression of abundant iGluR mRNAs. It is likely that higher expression of mRNA of genes involved in mitochondrial activity in the legs relative to the main bodies would be necessary to supply energy for leg movement.

In addition to iGluRs, the forelegs expressed high levels of transient receptor potential channel A1 as previously reported (Dong et al., 2017), anoctamin-7 (TMEM16 family), and two gustatory receptors (GRs): Tm03548 and Tm05586 (Dong et al., 2017) (**Supplementary Table S2** and **Figure 2**). Orthologs of these GRs were also present in *Ixodes scapularis*, but were not found in *D. melanogaster*, indicating that they are specifically expanded in the Acari lineage. Thus, the *T. mercedesae* sensory organ appears to be equipped with various sensory proteins with ion channel activity.

Conserved Sensory Functions Between *D. melanogaster* and *T. mercedesae* IR25a and IR93a

We previously annotated eight IR and 33 iGluR genes in the *T. mercedesae* genome and showed that two IR mRNAs, *Tm15229* and *Tm15231*, are abundantly expressed in the forelegs, using qRT-PCR (Dong et al., 2017). These two genes are included in the above DEGs and we also found that mRNAs for two non-NMDA iGluRs (Tm15234 and Tm15241), as well as two other IRs (Tm15230 and Tm15243), were also highly expressed in the forelegs (**Figure 2**). Thus, a small fraction of iGluRs and half of IRs appear to play roles in mite sensory perception.

Based on the phylogenetic tree of *T. mercedesae* IR and iGluR genes, together with those of *D. melanogaster* and *Ixodes*

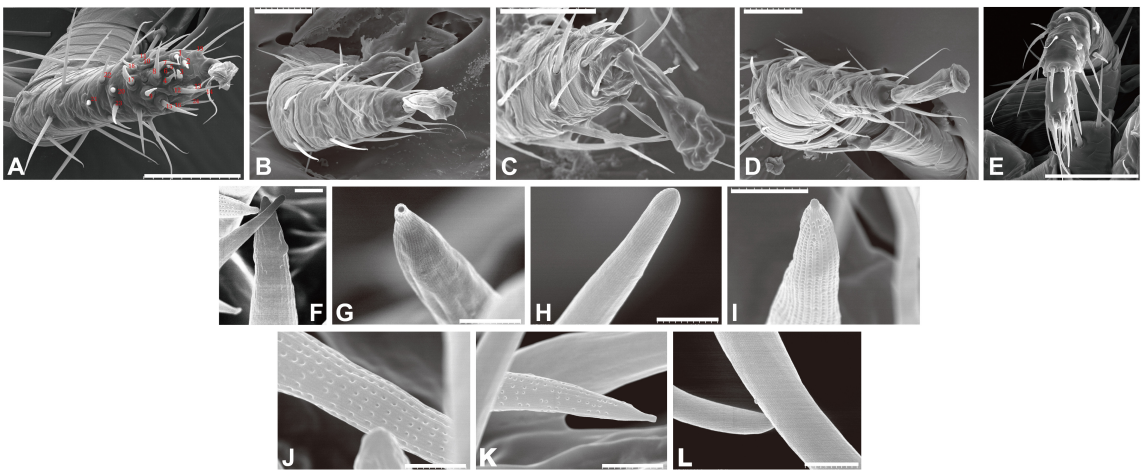

FIGURE 1 | Scanning electron micrographs of *Tropilaelaps mercedesae* sensory organ. **(A)** The foreleg with the numbered sensilla. **(B)** The second leg. **(C)** The third leg. **(D)** The fourth leg. **(E)** The pedipalp. **(F)** Sensillum #3 with a rough surface. **(G)** Sensillum #18 with a terminal pore. **(H)** Sensillum #8 with a smooth surface. **(I)** Sensillum #2 with surface pores of high density. **(J)** Sensillum #7 with surface pores of medium density. **(K)** Sensillum #10 with surface pores of low density. **(L)** Two sensilla at the distal end of pedipalp. A scale represents 50 μm in the panels **(A–E)**, 2 μm in the panels **(I,K)**, and 1 μm in the panels **(F–H,J,L)**.

TABLE 1 | GO terms enriched with genes highly expressed in the forelegs compared with hindlegs of *T. mercedesae.*

GO ID	GO name	GO category	FDR	*P*-value
GO:0005272	Sodium channel activity	Molecular function	1.83E-09	8.77E-13
GO:0004970	Ionotropic glutamate receptor activity	Molecular function	5.02E-06	1.05E-08
GO:0005234	Extracellularly glutamate-gated ion channel activity	Molecular function	0.00237124	1.68E-05
GO:0008527	Taste receptor activity	Molecular function	0.00237124	1.90E-05
GO:0008017	Microtubule binding	Molecular function	0.02302381	2.36E-04
GO:1990939	ATP-dependent microtubule motor activity	Molecular function	0.02706201	2.86E-04
GO:0006814	Sodium ion transport	Biological process	3.93E-07	3.78E-10
GO:0050912	Detection of chemical stimulus involved in sensory perception of taste	Biological process	0.00237124	1.90E-05
GO:1905515	Non-motile cilium assembly	Biological process	0.00237124	1.90E-05
GO:0042073	Intraciliary transport	Biological process	0.00237124	1.90E-05
GO:0010378	Temperature compensation of the circadian clock	Biological process	0.02706201	2.86E-04
GO:0030990	Intraciliary transport particle	Cellular component	0.00237124	1.90E-05
GO:0034464	BBSome	Cellular component	0.01633013	1.60E-04

scapularis (Dong et al., 2017), we found only two (out of eight) IRs (*Tm15229* and *Tm15231*) were conserved, having the *D. melanogaster* orthologs, *IR93a* and *IR25a*, respectively. DmIR93a and DmIR25a have been shown to play roles in temperature and humidity preferences (Enjin et al., 2016; Knecht et al., 2016; Ni et al., 2016). To test whether the sensory functions of IR93a and IR25a are deeply conserved between fruit flies and mites, we first obtained the full length cDNAs of *Tm15229* and *Tm15231* by determining both the 5′ and 3′ end sequences using RACE methods. Tm15229 (TmIR93a) and Tm15231 (TmIR25a) share the same protein domains with DmIR93a and DmIR25a, respectively (**Figure 3**). Tm/DmIR25a contains the N-terminal leucine/isoleucine/valine-binding protein (LIVBP)-like domain and PBP2_iGluR domain. Meanwhile, Tm/DmIR93a contained only the PBP2_iGluR domain. The protein expression was confirmed by ectopic expression in HEK293 cells, followed by western blot (**Supplementary Figure S1**). We then compared the thermotactic behavior of *D. melanogaster IR93a* and *IR93a* mutants expressing *TmIR93a* under *DmIR25a-Gal4* with the wild type. Expression of *DmIR93a* and *DmIR25a* overlapped in the antennae (Knecht et al., 2016). We also analyzed *D. melanogaster IR25a* and *IR25a* mutants expressing *DmIR25a* or *TmIR25a* under *DmIR25a-Gal4.* From our assay to test thermotactic behavior, the fraction of animals in the area with temperatures <24°C significantly increased in both *IR93a* and *IR25a* mutants compared with the wild type; however, expression of *TmIR93a*, *TmIR25a,* or *DmIR25a* rescued this behavioral defect (**Figure 4A**).

We then tested the humidity preferences of the fruit fly stocks described above. Wild type flies preferred high (saturated NaCl, 70%) over low (saturated LiCl, 20%) humidity but this preference was significantly impaired in *IR25a* and *IR93a* mutants (**Figure 4B**), as previously reported (Enjin et al., 2016; Knecht et al., 2016, 2017; Ni et al., 2016). Expression of *DmIR25a*

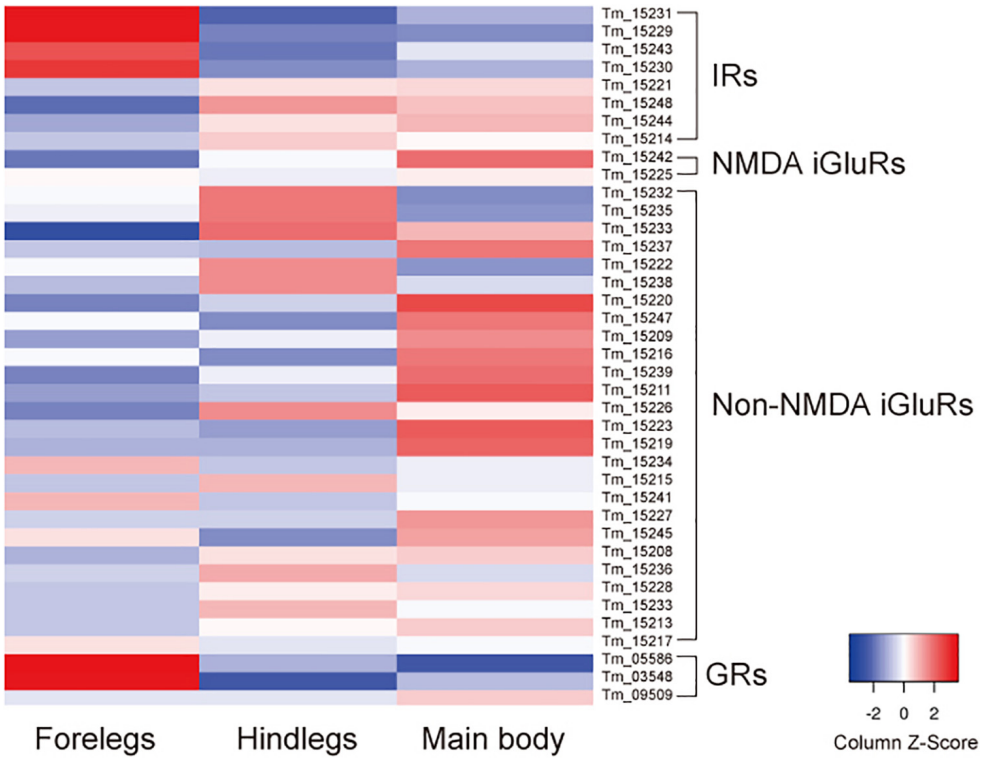

FIGURE 2 | Expression of ionotropic receptors (IRs), NMDA iGluRs, non-NMDA iGluRs, and gustatory receptors (GRs) mRNAs in the forelegs, hindlegs, and main body of *T. mercedesae*. The level of expression of each mRNA in the forelegs, hindlegs, and main body is shown by a graded color (blue to red) based on the counts per million mapped reads (CPM).

or *TmIR25a* was able to rescue the humidity preference defect of the mutant fly. Expression of *TmIR93a* partially rescued the defective phenotype of *IR93a* mutant and preference for 70% humidity of the rescued flies is significantly lower than that of wild type flies (**Figure 4B**).

We also examined whether *T. mercedesae* is capable of detecting ambient temperature and humidity and has the specific preferences. As shown in **Figure 5A**, the mites accumulated at the area of 32–40°C in a gradient of 15–40°C but randomly positioned on the testing arena without temperature gradient. Similarly, the mites were equally present on each side of the testing apparatus filled with H_2O (no humidity gradient); however, they accumulated on the side with H_2O (96% RH) over saturated LiCl (**Figure 5B**). These results demonstrate that the mites detect temperature as well as humidity and prefer 32–40°C and high humidity, which are equivalent to the inside environment of honey bee hive.

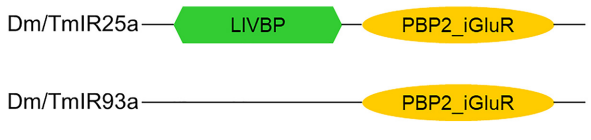

FIGURE 3 | Protein domains in Dm/TmIR25a and Dm/TmIR93a. Tm/DmIR25a contains a leucine/isoleucine/valine-binding protein (LIVBP)-like domain at the N-terminus and PBP2_iGluR domain (ligand-binding and ion channel domains) similar to iGluRs. Tm/DmIR93a contains only the PBP2_iGluR domain similar to other IRs.

DISCUSSION

Morphology and Structure of the *T. mercedesae* Sensory Organ

We aimed to identify a sensilla-rich sensory organ in the body of *T. mercedesae* using SEM and found two such organs, one on the pedipalp and the other on the dorsal side of the foreleg tarsus. The pedipalp contains a cluster of sensilla at the distal end; however, their morphology is uniform, suggesting that this sensory organ may perceive single type of stimulus. The sensory organ on the foreleg tarsus is comparable to Haller's organ in ticks, which is considered to be responsible for detecting humidity, temperature, and odor (Leonovich, 1990; Carr et al., 2017). Similar sensory organs have also been identified in the foreleg tarsi of the mites *Dermanyssus prognephilus* (Davis and Camin, 1976), *Dermanyssus gallinae* (Cruz et al., 2005), and *V. destructor* (Dillier et al., 2006; Häußermann et al., 2015). Thus, acarids are likely to share the same mechanisms for sensory perception. Nevertheless, structural diversity exists between different species. For example, *V. destructor* has nine large sensilla (R1-9) at the periphery and nine small sensilla (S1-9) on the inside of the

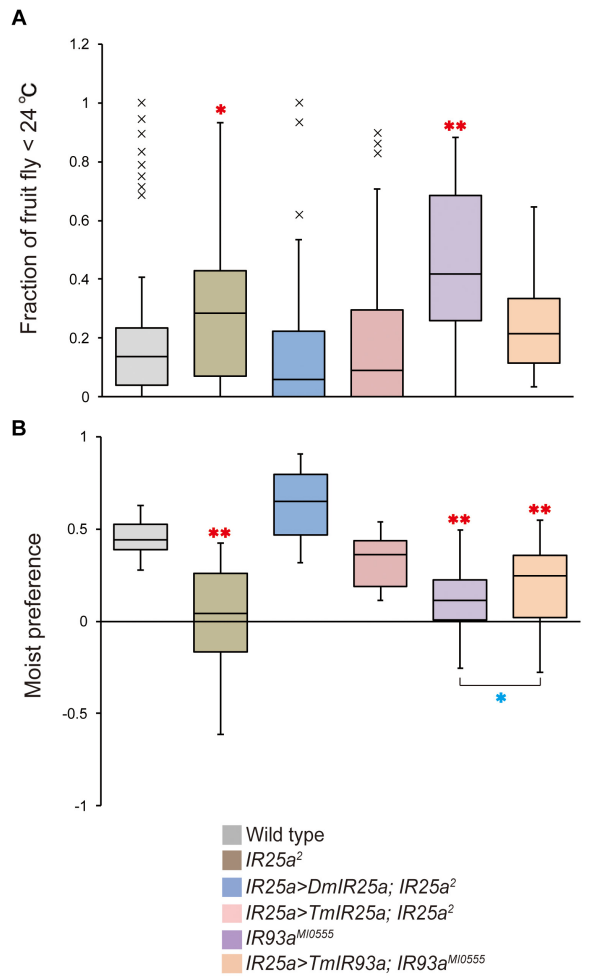

FIGURE 4 | *TmIR25a* and *TmIR93a* rescue the behavioral defects of *Drosophila melanogaster IR25a* and *IR93a* mutants. **(A)** The fraction of wild type (n = 108), $IR25a^2$ (n = 148), $IR25a^2$ expressing either *DmIR25a* (*IR25a > DmIR25a; IR25a*^{2}) (n = 63) or *TmIR25a* (*IR25a > TmIR25a; IR25a*^{2}) (n = 50), $IR93a^{MI0555}$ (n = 75), and $IR93a^{MI0555}$ expressing *TmIR93a* (*IR25a > TmIR93a; IR93a*^{MI0555}) (n = 60) under *IR25a-Gal4* in the area <24°C of the thermal gradient. Red asterisks (* and **) are significantly different from wild type, and P-values for $IR25a^2$ and $IR93a^{MI0555}$ are <0.03 and <0.001, respectively (two-tailed Dunnett test). **(B)** Moist preference (70 over 20% humidity) of fruit flies of above genotypes is shown (n = 39, 27, 9, 9, 39, 39 for wild type, $IR25a^2$, *IR25a > DmIR25a;* $IR25a^2$, *IR25a > TmIR25a;* $IR25a^2$, $IR93a^{MI0555}$, and *IR25a > TmIR93a;* $IR93a^{MI0555}$, respectively). Red asterisks (**) are significantly different from wild type (P-value < 0.001, two-tailed Dunnett test) and blue asterisk (*) indicates significant difference between $IR93a^{MI0555}$ and *IR25a > TmIR93a;* $IR93a^{MI0555}$ (P-value < 0.03, two-tailed Welch's t-test).

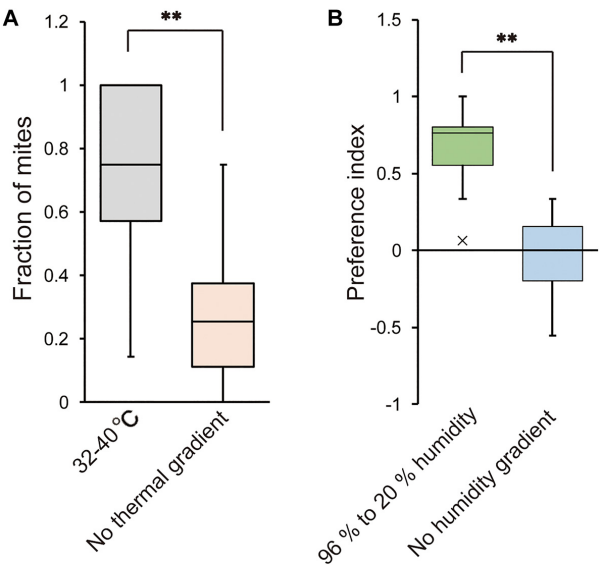

FIGURE 5 | Temperature and humidity preferences of *T. mercedesae*. **(A)** The fraction of mites in the area of 32–40°C (n = 18) and the same area but without thermal gradient (n = 21) is shown. Asterisk (**) indicates the significant difference between two groups (P-value < 0.001, two-tailed Welch's t-test). **(B)** Preference index of mites in the testing arena with 96% to 20% humidity (n = 20) and without humidity gradient (n = 12) is shown. Asterisk (**) indicates the significant difference between two groups (P-value < 0.001, two-tailed Welch's t-test).

sensory organ (Dillier et al., 2006; Häußermann et al., 2015). The sensory organ of *T. mercedesae* did not have such organization and the localization of small and long sensilla was also random (**Figure 1**). The existence of four different types of sensilla appears to be shared between *T. mercedesae* and *D. gallinae,* suggesting that the mite sensory organ could respond to mechanical stimuli, humidity, temperature, and compounds. Electrophysiological characterization of each sensillum is, of course, necessary to support this hypothesis.

T. mercedesae Sensory Organ Enriched With mRNAs for Sensory Proteins and Proteins Necessary for Ciliary Biogenesis/Transport

We sought to identify mRNAs differentially expressed in the forelegs of mites as candidates for those expressed in the sensory organs. Although we have no direct evidence to show that these mRNAs are indeed expressed in the sensory organ, their specific existence in the forelegs, as well as the identified DEGs, support this approach. The same method was used with two tick species, *Dermacentor variabilis* and *Ixodes scapularis*, to identify mRNAs associated with the Haller's organ (Mitchell et al., 2017; Josek et al., 2018). Our results to show the enrichment of *TmIR25a* and *TmIR93a* mRNAs in the forelegs of *T. mercedesae* are consistent with the results for *I. scapularis* (Josek et al., 2018). Eliash et al. (2017) also reported that the *V. destructor* homolog of IR25a (this may not be the ortholog since it does not have the N-terminal LIVBP domain) was highly expressed in the forelegs. These results suggest that IR25a and IR93a may represent the major thermo- and hygroreceptors in acarids, based on their physiological roles in fruit flies. This hypothesis was further supported by our finding that TmIR25a and TmIR93a rescued the defective thermo- and hygrosensation in *D. melanogaster IR25a* and *IR93a* mutants (**Figure 4**) and *T. mercedesae* is capable of

detecting ambient temperature and humidity (**Figure 5**). It is notable that not only the structure, but also the physiological roles, have been deeply conserved during Arthropod evolution (Croset et al., 2010). IR21a, IR40a, and IR68a are necessary for thermo- and hygrosensation together with IR25a and IR93a in *D. melanogaster* (Enjin et al., 2016; Knecht et al., 2016, 2017; Ni et al., 2016; Frank et al., 2017). However, as we previously reported, there are no orthologs of IR21a, IR40a, and IR68a in *T. mercedesae* genome. Two other IRs enriched in the mite foreleg are Tm15230 and Tm15243 which appear to be Acari-specific and the orthologs are absent in fruit fly. As the exclusive parasite of honey bee larva and pupa, *T. mercedesae* must adapt to the colony environment where the temperature and humidity are different and relatively constant compared to the outside environment. In fact, the mite prefers temperature between 32 and 40°C in contrast to *D. melanogaster* at 25°C. This may have resulted in evolving the novel IRs, Tm15230 and Tm15243, which are different from *D. melanogaster* IR21a, IR40a, and IR68a. However, the possibility that Tm15230 and Tm15243 are involved in chemosensation cannot be ruled out at this stage. Two (Tm03548 and Tm05586) and eight GR mRNAs were highly expressed in the sensory organs of *T. mercedesae* and *I. scapularis*, respectively (Josek et al., 2018). However, these GRs do not appear to be orthologs and Josek et al. (2018) reported that the expression of other *I. scapularis* GRs was too low to make a comparison between the forelegs and hindlegs. Furthermore, most of the GRs have expanded in Acari in a lineage-specific manner (Eyun et al., 2017; Josek et al., 2018). Except for Gr28b in *D. melanogaster,* which has an important role in thermosensation (Ni et al., 2013), GRs are generally considered to function as chemoreceptors. Thus, the above two GRs of *T. mercedesae* may detect, for example, a few odorants/tastants derived from honey bee adults, larva, and larval food. This is consistent with the finding that the numbers of IR and GR genes in parasitic *T. mercedesae* were dramatically reduced compared to those in "free-living" mites/ticks (Dong et al., 2017). The TRPA1 channel was also enriched in the forelegs and may function as a sensor to detect nociceptive stimuli (temperature and chemicals) for avoidance, as previously reported (Peng et al., 2015, 2016; Dong et al., 2016). In summary, *T. mercedesae* may depend on IR25a, IR93a, and TRPA1 for thermosensation, IR25a and IR93a for hygrosensation, and two acarid-specific GRs (Tm03548 and Tm05586) as well as TRPA1 for chemosensation. It is difficult to extrapolate the precise physiological roles of two acarid-specific IRs (Tm15230 and Tm15243) at this stage.

Another group of proteins enriched in the forelegs is associated with cilium assembly and intraciliary transport processes and includes kinesin, dynein, and intraflagellar transport proteins. Cilia are organelles present on the cell surface that concentrate signaling molecules to organize sensory, developmental, and homeostatic function. Movement of the signaling receptor from the basal body into the cilia requires IFT-A and its exit depends on IFT-B and BBSome (Nachury, 2018). Many sensilla are present in the sensory organ of *T. mercedesae* (**Figure 1**) and sensory neurons associated with the sensilla have a ciliated dendrite, which requires the protein complexes described above to control traffic of, for example, sensory proteins. GPCRs are considered to be the major target for intraciliary transport (Schou et al., 2015); however, the four IRs of *T. mercedesae* may also depend on IFT-A, IFT-B, BBSome, and other proteins for transport. Consistent with the presence of few sensilla in the Haller's organs of two tick species, enrichment of these mRNAs was not observed (Carr et al., 2017). In contrast to Carr et al. (2017), we did not observe high expression of mRNAs for the downstream signaling pathway components of sensory proteins in the forelegs of *T. mercedesae*.

Our study uncovers the ancient roles of IR25a and IR93a in thermo- and hygrosensation of arthropods. We also found the potential roles of evolutionarily conserved intraciliary transport proteins for the entry and exit of sensory proteins in the ciliated dendrites of sensory neurons. The functional disruption of these proteins could be considered as an effective method to control honey bee parasitic mites as well as other mites/ticks that represent major pests for plants and animals.

AUTHOR CONTRIBUTIONS

JL and QL conducted the experiments. TK supervised the research project and wrote the manuscript with JL.

FUNDING

This work was supported by Jinji Lake Double Hundred Talents Programme to TK.

ACKNOWLEDGMENTS

We thank Bloomington Stock Center for providing us fruit fly stocks for the experiments. We are grateful to Xinyi Li for sampling the mites and Ziwen Xie for preparing the fruit fly food. This manuscript has been released as a pre-print at bioRxiv.

SUPPLEMENTARY MATERIAL

The Supplementary Material for this article can be found online at: https://www.frontiersin.org/articles/10.3389/fphys.2019.00556/full#supplementary-material

FIGURE S1 | Expression of TmIR25a and TmIR93a proteins. The IR proteins (V5-epitope) and β-actin expressed in HEK293 cells transfected with empty vector (Mock), TmIR25a-, and TmIR93a-expressing constructs were analyzed by western blot. The size (kDa) of protein molecular weight marker (MW) is at the left.

TABLE S1 | Total reads of RNA-seq and the alignment rates to the reference genome.

TABLE S2 | List of genes highly expressed in the forelegs relative to hindlegs.

TABLE S3 | List of genes highly expressed in the forelegs relative to main body.

TABLE S4 | List of genes highly expressed in the hindlegs relative to main body.

TABLE S5 | GO terms enriched with genes highly expressed in the forelegs compared with main bodies of *T. mercedesae.*

TABLE S6 | GO terms enriched with genes highly expressed in the hindlegs compared with main bodies of *T. mercedesae.*

REFERENCES

Aizen, M. A., and Harder, L. D. (2009). The global stock of domesticated honey bees is growing slower than agricultural demand for pollination. *Curr. Biol.* 19, 915–918. doi: 10.1016/j.cub.2009.03.071

Anders, S., Pyl, P. T., and Huber, W. (2015). HTSeq–a Python framework to work with high-throughput sequencing data. *Bioinformatics* 31, 166–169.

Anderson, D., and Roberts, J. (2013). Standard methods for *Tropilaelaps* mites research. *J. Apic. Res.* 52, 1–16.

Anderson, D. L., and Morgan, M. J. (2007). Genetic and morphological variation of bee-parasitic *Tropilaelaps* mites (Acari: Laelapidae): new and re-defined species. *Exp. Appl. Acarol.* 43, 1–24.

Aumeier, P., Rosenkranz, P., and Francke, W. (2002). Cuticular volatiles, attractivity of worker larvae and invasion of brood cells by *Varroa* mites. A comparison of Africanized and European honey bees. *Chemoecology* 12, 65–75.

Belozerov, V., Kok, D., and Fourie, L. J. (1997). Regeneration of Haller's sensory organ in the tick, Ixodes rubicundus (Acari: Ixodidae). *Exp. Appl. Acarol.* 21, 629–648.

Benton, R., Vannice, K. S., Gomez-Diaz, C., and Vosshall, L. B. (2009). Variant ionotropic glutamate receptors as chemosensory receptors in *Drosophila*. *Cell* 136, 149–162. doi: 10.1016/j.cell.2008.12.001

Brand, A. H., and Perrimon, N. (1993). Targeted gene expression as a means of altering cell fates and generating dominant phenotypes. *Development* 118, 401–415.

Carr, A. L., Mitchell, R. D. III., Dhammi, A., Bissinger, B. W., Sonenshine, D. E., and Roe, R. M. (2017). Tick haller's organ, a new paradigm for arthropod olfaction: how ticks differ from insects. *Int. J. Mol. Sci.* 18:1563. doi: 10.3390/ijms18071563

Conesa, A., Götz, S., García-Gómez, J. M., Terol, J., Talón, M., and Robles, M. (2005). Blast2GO: a universal tool for annotation, visualization and analysis in functional genomics research. *Bioinformatics* 21, 3674–3676.

Croset, V., Rytz, R., Cummins, S. F., Budd, A., Brawand, D., Kaessmann, H., et al. (2010). Ancient protostome origin of chemosensory ionotropic glutamate receptors and the evolution of insect taste and olfaction. *PLoS Genet.* 6:e1001064. doi: 10.1371/journal.pgen.1001064

Cruz, M. D. S., Vega Robles, M. C., Jespersen, J. B., Kilpinen, O., Birkett, M., Dewhirst, S., et al. (2005). Scanning electron microscopy of foreleg tarsal sense organs of the poultry red mite, *Dermanyssus gallinae* (DeGeer) (Acari:Dermanyssidae). *Micron* 36, 415–421.

Dainat, B., Evans, J. D., Chen, Y. P., Gauthier, L., and Neumann, P. (2012). Dead or alive: deformed wing virus and *Varroa destructor* reduce the life span of winter honeybees. *Appl. Environ. Microbiol.* 78, 981–987. doi: 10.1128/AEM.06537-11

Dainat, B., Ken, T., Berthoud, H., and Neumann, P. (2009). The ectoparasitic mite *Tropilaelaps mercedesae* (Acari, Laelapidae) as a vector of honeybee viruses. *Insectes Soc.* 56, 40–43.

Davis, J. C., and Camin, J. H. (1976). Setae of the anterior tarsi of the martin mite, *Dermanyssus prognephilus* (Acari: Dermanyssidae). *J. Kans. Entomol. Soc.* 49, 441–449.

de Miranda, J. R., and Genersch, E. (2010). Deformed wing virus. *J. Invertebr. Pathol.* 103, S48–S61. doi: 10.1016/j.jip.2009.06.012

Dillier, F. X., Fluri, P., and Imdorf, A. (2006). Review of the orientation behaviour in the bee parasitic mite *Varroa destructor*: sensory equipment and cell invasion behaviour. *Rev. Suisse Zool.* 113, 857–877.

Dong, X., Armstrong, S. D., Xia, D., Makepeace, B. L., Darby, A. C., and Kadowaki, T. (2017). Draft genome of the honey bee ectoparasitic mite, *Tropilaelaps mercedesae*, is shaped by the parasitic life history. *GigaScience* 6, 1–17. doi: 10.1093/gigascience/gix008

Dong, X., Kashio, M., Peng, G., Wang, X., Tominaga, M., and Kadowaki, T. (2016). Isoform-specific modulation of the chemical sensitivity of conserved TRPA1 channel in the major honeybee ectoparasitic mite, *Tropilaelaps mercedesae*. *Open Biol.* 6:160042. doi: 10.1098/rsob.160042

Eliash, N., Singh, N. K., Thangarajan, S., Sela, N., Leshkowitz, D., Kamer, Y., et al. (2017). Chemosensing of honeybee parasite, *Varroa destructor*: transcriptomic analysis. *Sci. Rep.* 7:13091. doi: 10.1038/s41598-017-13167-9

Enjin, A., Zaharieva, E. E., Frank, D. D., Mansourian, S., Suh, G. S. B., Gallio, M., et al. (2016). Humidity sensing in *Drosophila*. *Curr. Biol.* 26, 1352–1358. doi: 10.1016/j.cub.2016.03.049

Evans, J. D., and Schwarz, R. S. (2011). Bees brought to their knees: microbes affecting honey bee health. *Trends Microbiol.* 19, 614–620. doi: 10.1016/j.tim.2011.09.003

Eyun, S.-I., Soh, H. Y., Posavi, M., Munro, J. B., Hughes, D. S. T., Murali, S. C., et al. (2017). Evolutionary history of chemosensory-related gene families across the arthropoda. *Mol. Biol. Evol.* 34, 1838–1862. doi: 10.1093/molbev/msx147

Forsgren, E., de Miranda, J. R., Isaksson, M., Wei, S., and Fries, I. (2009). Deformed wing virus associated with *Tropilaelaps mercedesae* infesting European honey bees (*Apis mellifera*). *Exp. Appl. Acarol.* 47, 87–97. doi: 10.1007/s10493-008-9204-4

Frank, D. D., Enjin, A., Jouandet, G. C., Zaharieva, E. E., Para, A., Stensmyr, M. C., et al. (2017). Early integration of temperature and humidity stimuli in the *Drosophila* brain. *Curr Biol. CB* 27:2381-2388.e4. doi: 10.1016/j.cub.2017.06.077

Goulson, D., Nicholls, E., Botías, C., and Rotheray, E. L. (2015). Bee declines driven by combined stress from parasites, pesticides, and lack of flowers. *Science* 347:1255957. doi: 10.1126/science.1255957

Häußermann, C. K., Ziegelmann, B., Bergmann, P., and Rosenkranz, P. (2015). Male mites (*Varroa destructor*) perceive the female sex pheromone with the sensory pit organ on the front leg tarsi. *Apidologie* 46, 771–778.

Iovinella, I., McAfee, A., Mastrobuoni, G., Kempa, S., Foster, L. J., Pelosi, P., et al. (2018). Proteomic analysis of chemosensory organs in the honey bee parasite *Varroa destructor*: a comprehensive examination of the potential carriers for semiochemicals. *J. Proteom.* 181, 131–141. doi: 10.1016/j.jprot.2018.04.009

Josek, T., Walden, K. K. O., Allan, B. F., Alleyne, M., and Robertson, H. M. (2018). A foreleg transcriptome for *Ixodes scapularis* ticks: candidates for chemoreceptors and binding proteins that might be expressed in the sensory Haller's organ. *Ticks Tick Borne Dis.* 9, 1317–1327.

Khongphinitbunjong, K., Neumann, P., Chantawannakul, P., and Williams, G. R. (2016). The ectoparasitic mite *Tropilaelaps mercedesae* reduces western honey bee, *Apis mellifera*, longevity and emergence weight, and promotes deformed wing virus infections. *J. Invertebr. Pathol.* 137, 38–42. doi: 10.1016/j.jip.2016.04.006

Kim, D., Langmead, B., and Salzberg, S. L. (2015). HISAT: a fast spliced aligner with low memory requirements. *Nat. Methods* 12, 357–360. doi: 10.1038/nmeth.3317

Klein, A. M., Vaissière, B. E., Cane, J. H., Steffan-Dewenter, I., Cunningham, S. A., Kremen, C., et al. (2007). Importance of pollinators in changing landscapes for world crops. *Proc. Biol. Sci.* 274, 303–313.

Knecht, Z. A., Silbering, A. F., Cruz, J., Yang, L., Croset, V., Benton, R., et al. (2017). Ionotropic Receptor-dependent moist and dry cells control hygrosensation in *Drosophila*. *eLife* 6:e26654. doi: 10.7554/eLife.26654

Knecht, Z. A., Silbering, A. F., Ni, L., Klein, M., Budelli, G., Bell, R., et al. (2016). Distinct combinations of variant ionotropic glutamate receptors mediate thermosensation and hygrosensation in *Drosophila*. *eLife* 5:e17879. doi: 10.7554/eLife.17879

Kraus, B. (1993). Preferences of Varroa jacobsoni for honey bees (*Apis mellifera* L.) of different ages. *J. Apic. Res.* 32, 57–64.

Le Conte, Y., and Arnold, G. (1987). Influence de l'age des abeilles et de la chaleur sur le comportement de *Varroa jacobsoni*. *Apidologie* 18, 305–320.

Le Conte, Y., and Arnold, G. (1988). Etude du thermopreferendum de *Varroa jacobsoni* Oud. *Apidologie* 19, 155–164.

Le Conte, Y., Arnold, G., and Desenfant, P. (1990). Influence of brood temperature and hygrometry variations on the development of the honey bee ectoparasite *Varroa jacobsoni* (Mesostigmata: Varroidae). *Environ. Entomol.* 19, 1780–1785.

Leonovich, S. A. (1990). "Fine structural features of sensory systems in ticks and mites: evolutionary and ethological aspects," in *Sensory Systems and Communication in Arthropods*, eds F. G. Gribakin, K. Wiese, and A. V. Popov (Basel: Birkhäuser), 44–48. doi: 10.1007/978-3-0348-6410-7_8

Li, H., Handsaker, B., Wysoker, A., Fennell, T., Ruan, J., Homer, N., et al. (2009). The sequence alignment/map format and SAMtools. *Bioinformatics* 25, 2078–2079. doi: 10.1093/bioinformatics/btp352

Luo, Q. H., Zhou, T., Dai, P. L., Song, H. L., Wu, Y. Y., and Wang, Q. (2011). Prevalence, intensity and associated factor analysis of *Tropilaelaps mercedesae* infesting *Apis mellifera* in China. *Exp. Appl. Acarol.* 55, 135–146. doi: 10.1007/s10493-011-9459-z

Martin, S. J., Highfield, A. C., Brettell, L., Villalobos, E. M., Budge, G. E., Powell, M., et al. (2012). Global honey bee viral landscape altered by a parasitic mite. *Science* 336, 1304–1306. doi: 10.1126/science.1220941

Mitchell, R. D. III., Zhu, J., Carr, A. L., Dhammi, A., Cave, G., Sonenshine, D. E., et al. (2017). Infrared light detection by the haller's organ of adult american dog ticks, *Dermacentor* variabilis (Ixodida: Ixodidae). *Ticks Tick Borne Dis.* 8, 764–771. doi: 10.1016/j.ttbdis.2017.06.001

Nachury, M. V. (2018). The molecular machines that traffic signaling receptors into and out of cilia. *Curr. Opin. Cell Biol* 51, 124–131. doi: 10.1016/j.ceb.2018.03.004

Nazzi, F., and Conte, Y. L. (2016). Ecology of *Varroa destructor*, the major ectoparasite of the western honey bee, *Apis mellifera*. *Annu. Rev. Entomol.* 61, 417–432. doi: 10.1146/annurev-ento-010715-023731

Nazzi, F., and Le Conte, Y. (2016). Ecology of *Varroa destructor*, the major ectoparasite of the western honey bee, *Apis mellifera*. *Annu. Rev. Entomol.* 61, 417–432. doi: 10.1146/annurev-ento-010715-023731

Ni, L., Bronk, P., Chang, E. C., Lowell, A. M., Flam, J. O., Panzano, V. C., et al. (2013). A gustatory receptor paralogue controls rapid warmth avoidance in *Drosophila*. *Nature* 500, 580–584. doi: 10.1038/nature12390

Ni, L., Klein, M., Svec, K. V., Budelli, G., Chang, E. C., Ferrer, A. J., et al. (2016). The ionotropic receptors IR21a and IR25a mediate cool sensing in *Drosophila*. *eLife* 5:e13254. doi: 10.7554/eLife.13254

Peng, G., Kashio, M., Li, T., Dong, X., Tominaga, M., and Kadowaki, T. (2016). TRPA1 channels in *Drosophila* and honey bee ectoparasitic mites share heat sensitivity and temperature-related physiological functions. *Front. Physiol.* 7:447. doi: 10.3389/fphys.2016.00447

Peng, G., Kashio, M., Morimoto, T., Li, T., Zhu, J., Tominaga, M., et al. (2015). Plant-derived tick repellents activate the honey bee ectoparasitic mite TRPA1. *Cell Rep.* 12, 190–202. doi: 10.1016/j.celrep.2015.06.025

Robinson, M. D., McCarthy, D. J., and Smyth, G. K. (2010). edgeR: a Bioconductor package for differential expression analysis of digital gene expression data. *Bioinformatics* 26, 139–140. doi: 10.1093/bioinformatics/btp616

Rosenkranz, P., Aumeier, P., and Ziegelmann, B. (2010). Biology and control of *Varroa destructor*. *J. Invertebr. Pathol.* 103, S96–S119. doi: 10.1016/j.jip.2009.07.016

Rytz, R., Croset, V., and Benton, R. (2013). Ionotropic receptors (IRs): chemosensory ionotropic glutamate receptors in *Drosophila* and beyond. *Insect Biochem. Mol. Biol.* 43, 888–897. doi: 10.1016/j.ibmb.2013.02.007

Sammataro, D., Gerson, U., and Needham, G. (2000). Parasitic mites of honey bees: life history, implications, and impact. *Annu. Rev. Entomol.* 45, 519–548.

Sayeed, O., and Benzer, S. (1996). Behavioral genetics of thermosensation and hygrosensation in *Drosophila*. *Proc. Natl. Acad. Sci. U.S.A.* 93, 6079–6084. doi: 10.1073/pnas.93.12.6079

Schou, K. B., Pedersen, L. B., and Christensen, S. T. (2015). Ins and outs of GPCR signaling in primary cilia. *EMBO Rep.* 16, 1099–1113. doi: 10.15252/embr.201540530

Wu, Y., Dong, X., and Kadowaki, T. (2017). Characterization of the copy number and variants of deformed wing virus (DWV) in the pairs of honey bee pupa and infesting *Varroa destructor* or *Tropilaelaps mercedesae*. *Front. Microbiol.* 8:1558. doi: 10.3389/fmicb.2017.01558

Xie, X., Huang, Z. Y., and Zeng, Z. (2016). Why do *Varroa* mites prefer nurse bees? *Sci. Rep.* 6:28228. doi: 10.1038/srep28228

Yue, C., and Genersch, E. (2005). RT-PCR analysis of deformed wing virus in honeybees (*Apis mellifera*) and mites (*Varroa destructor*). *J. Gen. Virol.* 86, 3419–3424.

Conflict of Interest Statement: The authors declare that the research was conducted in the absence of any commercial or financial relationships that could be construed as a potential conflict of interest.